Research Article

Effect of Initial Orientation on the Laser-Induced Cycloaddition Reaction of Benzene and Ethylene

Shuai Yuan,[1] Huiling Hong,[1] Gang Wang,[1] Wenying Zhang,[1] Weifeng Wu,[1] Yusheng Dou,[2] and Glenn V. Lo[2]

[1] *School of Bioinformation, Chongqing University of Posts and Telecommunications, Chongqing 400065, China*
[2] *Department of Physical Sciences, Nicholls State University, P.O. Box 2022, Thibodaux, LA 70310, USA*

Correspondence should be addressed to Shuai Yuan; yuanshuai@cqupt.edu.cn and Yusheng Dou; yusheng.dou@nicholls.edu

The [2 + 2] photocycloaddition reaction of benzene and ethylene was investigated by semiclassical dynamics simulation and complete active space self-consistent field (CASSCF) *ab initio* calculations. Following laser excitation of the benzene molecule, two mechanisms were observed depending on the location of the second C of ethylene in relation to the hexagonal prism space defined by the first C and the plane of the benzene ring. Synchronous formation of two bonds was observed when the second C is outside the prism space; an asynchronous mechanism is observed otherwise. Charge transfer was observed only in the asynchronous mechanism; CASSCF calculations suggest that the asynchronous mechanism involves a barrierless path from the Frank-Condon point to a conical intersection, while the synchronous mechanism involves 0.8 eV barrier. These results are consistent with a higher quantum yield observed in the simulations for the asynchronous pathway.

1. Introduction

A photocycloaddition reaction is a light-induced reaction that forms a new molecule from two unsaturated molecules via two atoms from each molecule. These reactions are "atom-economical" and "step-economical"; all the atoms in the reactants appear in the products and complexity can be achieved in a single step [1, 2]. With unprecedented possibilities to efficiently create various new molecules, photocycloadditions are widely applied in organic synthesis. A photocycloaddition reaction between benzene (or its derivatives) and an alkene can be classified into three types: [2 + 2] (or *ortho*), [3 + 2] (or *meta*), and [4 + 2] (or *para*). Photocycloadditions of benzene and an alkene are usually induced by the photoexcitation of the benzene molecule. If the S_1 state of benzene is involved, only the *meta*-addition mode is allowed to occur in a concerted fashion (i.e., synchronous formation of two single bonds) according to molecular orbital symmetry rules [3, 4]. The formation of *ortho*- and *para*-cycloadducts can be interpreted as being due to charge transfer, a nonconcerted mechanism, or the involvement of the S_2 excited state.

Robb's group has conducted theoretical studies of the photocycloaddition of benzene and ethylene system using CASSCF calculation and MMVB simulation [5]. They found that such reactions could occur from S_1 state barrierless through a conical intersection (CI), which is shared by all three photocycloaddition products. This low energy CI follows the formation of one C–C bond between benzene and ethylene. Subsequent studies [6] suggest that the chemical selectivity is, in part, controlled by this extended conical intersection seam and that the shape of the conical intersection seam can be understood in terms of simple VB arguments. Further, the shape and energetics of the asynchronous segment of the conical intersection seam suggest that the 1,2 (*ortho*) and 1,3 (*meta*) products are equally preferred. The 1,4 (*para*) point on the conical intersection is higher in energy and corresponds to a local maximum on the seam.

In this paper, we describe the results of semiclassical dynamics simulations of photoinduced [2 + 2] cycloaddition of benzene and ethylene. Specifically, we investigated the effect of the stacking orientation at the moment of laser excitation of the benzene molecule on the subsequent

$\delta(8\text{-}7\text{-}1\text{-}2) = 38.2°$

(a)
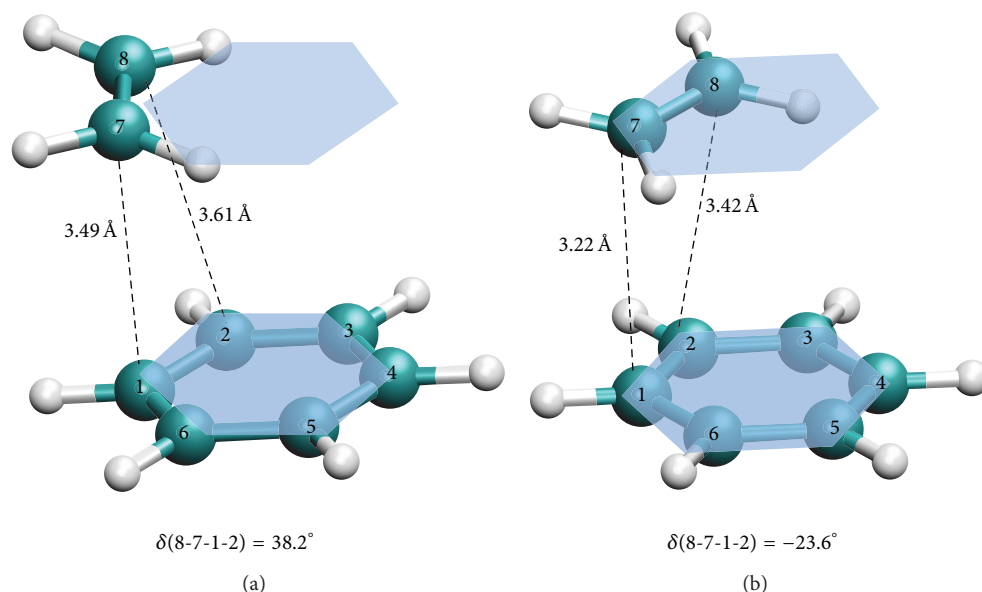
$\delta(8\text{-}7\text{-}1\text{-}2) = -23.6°$

(b)

FIGURE 1: (a) The equilibrated Geometry I and (b) equilibrated Geometry II of the benzene plus ethylene molecule with atomic labeling. Shadows herein indicate hypothetical hexagonal prism space of upward projection of benzene molecule.

dynamics. Previous studies on stacked DNA base molecules have shown that the initial orientation of reactant molecules affects the excited state dynamics [7–10]. Our simulations provide detailed dynamics features from photon excitation to the formation of product. The results are interpreted in terms of the geometry of conical intersection (CI) between the first singlet (S_1) excited state and ground state (S_0), which was optimized by using CASSCF method.

2. Methodology

2.1. Semiclassical Dynamics Simulation. We carried out the dynamics simulations using the semiclassical electron-radiation-ion dynamics (SERID) method. A detailed description of this technique has been published elsewhere [11, 12] and only a brief review is given here. In this approach, the valence electrons are calculated by the time-dependent Schrödinger equation while both the radiation field and the motion of the nuclei are treated by the classical approximation. The one-electron states are updated by solving the time-dependent Schrödinger equation at each time step (typically 0.05 femtoseconds in duration) on a nonorthogonal basis using a unitary algorithm obtained from the equation for the time evolution operator [13]. The laser pulse is characterized by the vector potential **A**, which is coupled to the Hamiltonian via the time-dependent Peierls substitution [14]. The Hamiltonian matrix elements, overlap matrix elements, and repulsive energy are calculated with the density-functional based tight bonding (DFTB) method [15, 16]. The DFTB method does have essentially the same strengths and limitations as time-dependent density-functional theory (TD-DFT). In particular, the bonding is well-described, but the excited-state energies are typically too low. For this reason, we matched the effective central photon energy of the laser pulse

to the relevant density-functional (rather than experimental) excitation energy and this should not affect the interpretation of the results. In this technique, forces acting on nucleus or ions are computed by the Ehrenfest equation, which is obtained by neglecting the terms of second and higher order in the quantum fluctuations in the exact Ehrenfest theorem. The nuclear motion is numerically integrated with the velocity Verlet algorithm (which preserves phase space). A time step of 50 attoseconds was used based on the test of energy conservation.

The SERID method has been used in biologically relevant studies such as photoinduced dimerization of thymine [9] and cytosine [10] via [2 + 2] photocycloaddition reaction. All the results were found to be consistent with experimental observations. The formation of cyclobutane pyrimidine dimer may provide good references for [2 + 2] photocycloaddition of benzene and ethylene.

2.2. CASSCF. Multiconfigurational self-consistent field (MCSCF) is a method in quantum chemistry used to generate qualitatively correct reference states of molecules in cases where Hartree-Fock (HF) and DFT are not adequate (e.g., for molecular ground states which are quasi-degenerate with low-lying excited states or in bond breaking situations). It uses a linear combination of configuration state functions (CSF) or configuration determinants to approximate the exact electronic wavefunction of an atom or molecule. In an MCSCF calculation, the set of coefficients of both the CSFs or determinants and the basis functions in the molecular orbitals are varied to obtain the total electronic wavefunction with the lowest possible energy. This method can be considered a combination of configuration interaction (where the molecular orbitals are not varied but the expansion of the wave function) and Hartree-Fock (where

(a) $t = 0$ fs

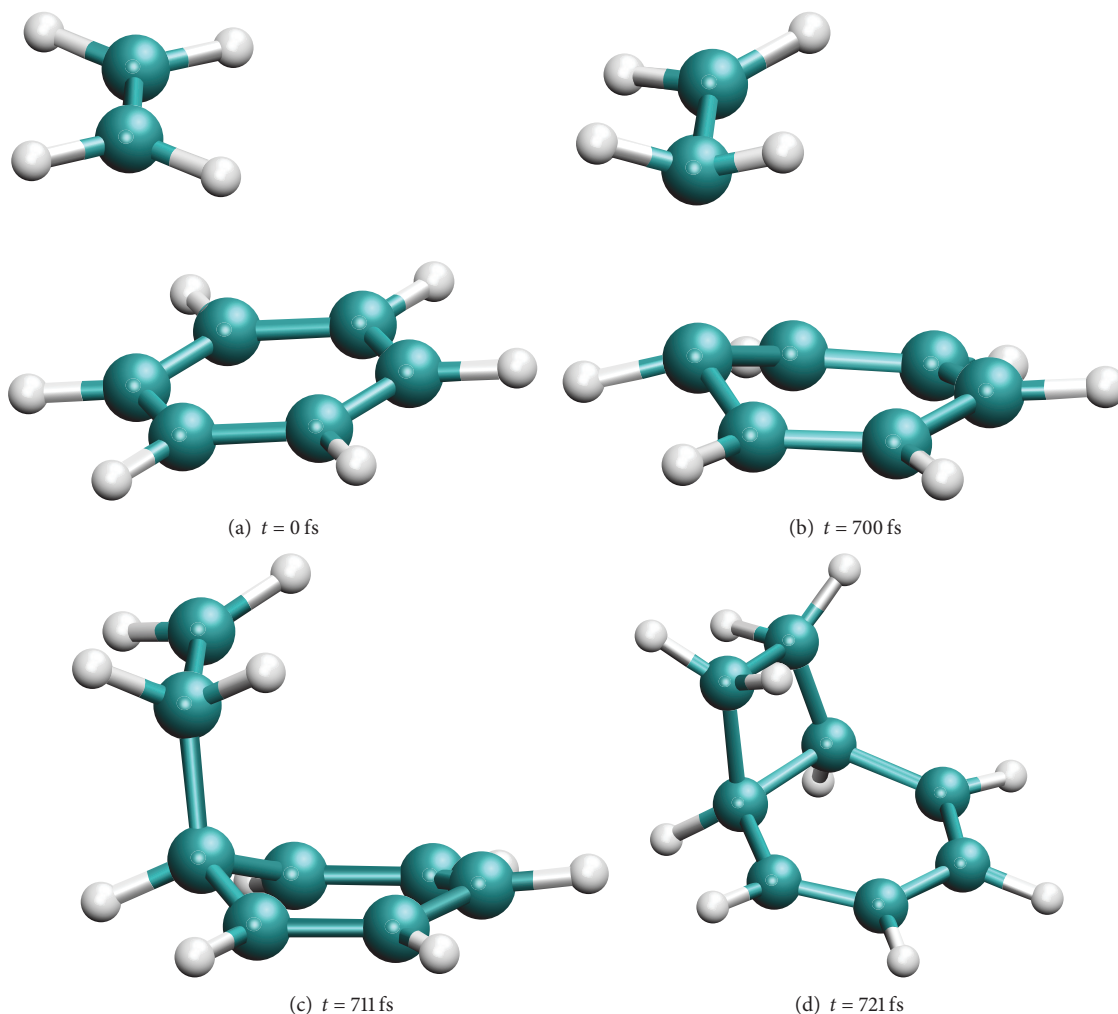(b) $t = 700$ fs

(c) $t = 711$ fs

(d) $t = 721$ fs

Figure 2: Snapshots taken from the simulation of synchronous cycloaddition mode of stacked benzene and ethylene molecules at (a) 0, (b) 700, (c) 711, and (d) 721 fs. The benzene molecule is subjected to the irradiation of a 25 fs (fwhm) laser pulse with a fluence of 96.93 J·m^{-2} and photon energy of 4.7 eV.

there is only one determinant but the molecular orbitals are varied). A particularly important MCSCF approach is the CASSCF method, where the linear combination of CSFs includes all that arises from a particular number of electrons in a particular number of orbitals [17, 18].

In this research, the CASSCF computations used an 8-electron and 8-orbital active space involving all the π orbitals of benzene and ethylene moieties. All the geometries were optimized using the 6-31G(d) basis set in Gaussian 09 [19].

3. Results and Discussion

To obtain a ground state initial configuration, the simulation was run at room temperature for 1000 fs starting with a randomly stacked geometry of benzene and ethylene. During this equilibration period, one hundred geometries were taken at equal time intervals; each geometry was subjected to a laser pulse. Figure 1 shows two representative geometries, at the moment of excitation, that lead to two different mechanisms.

In Figure 1(a), the ethylene molecule was placed in such a way that $C_1–C_7 = 3.49$ Å, $C_2–C_8 = 3.61$ Å, and dihedral angle $C_8–C_7–C_1–C_2 = 38.2°$ (Geometry I); the carbon atoms in the ethylene molecule are numbered C_7 and C_8. The C_8 atom sticks out of the hexagonal prism defined by a vertical projection of benzene molecule (as indicated by the two shadows) through C_7. In Figure 1(b), benzene and ethylene molecule are oriented as follows: $C_1–C_7 = 3.22$ Å, $C_2–C_8 = 3.42$ Å, and dihedral angle $C_8–C_7–C_1–C_2 = −23.6°$ (Geometry II). The negative dihedral angle suggests that the C_8 atom of ethylene molecule is in the hypothetical hexagonal prism space.

A 25 fs FWHM laser pulse with a Gaussian profile, with photon energy of 4.7 eV, was applied to this complex. A fluence between 0.07 and 0.15 kJ·m^{-2} was chosen for this study. Within this range, effective electronic excitation occurs, but the forces produced do not break any bonds. The 100 trajectories show that Geometry I would lead to synchronous addition and asynchronous mode frequently

(a) $t = 0$ fs

(b) $t = 600$ fs

(c) $t = 655$ fs

(d) $t = 925$ fs

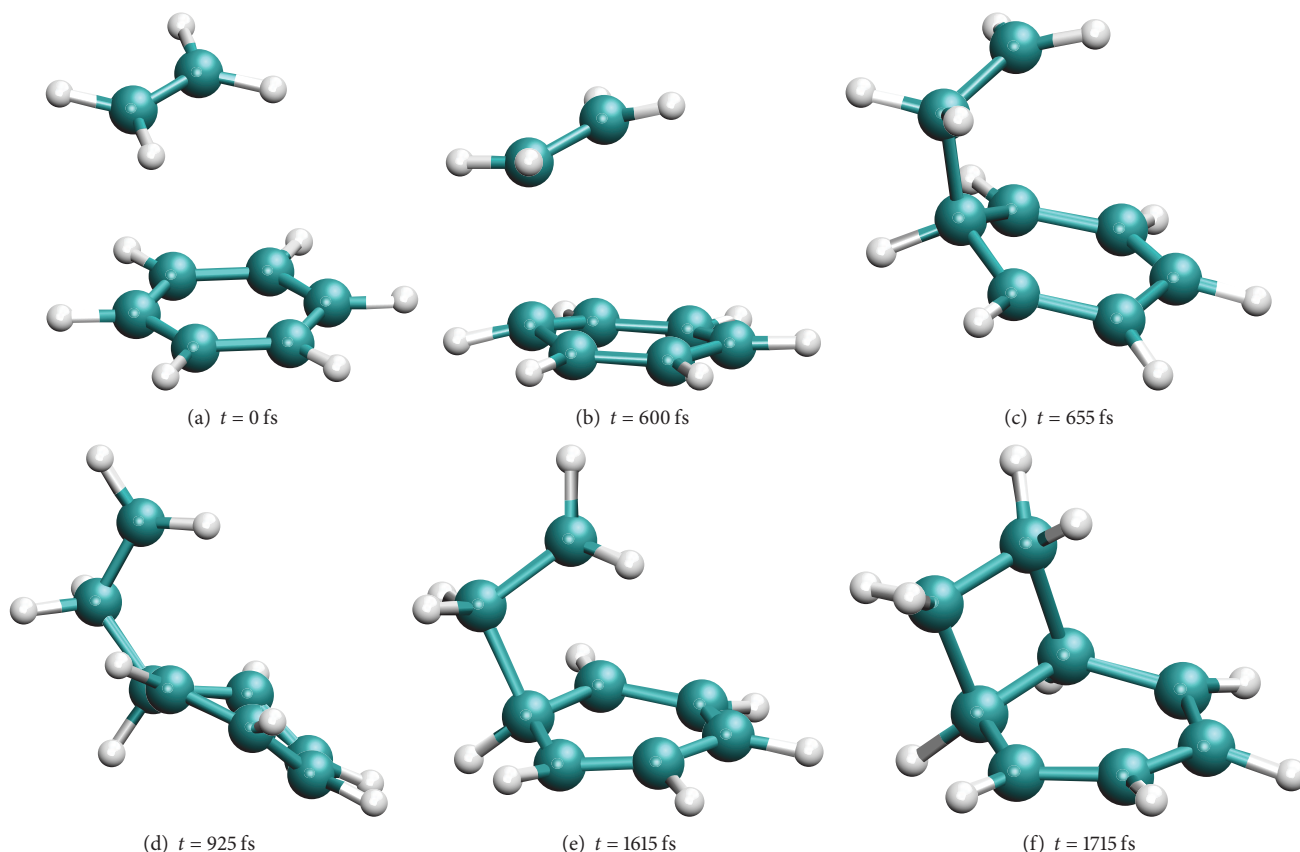(e) $t = 1615$ fs

(f) $t = 1715$ fs

Figure 3: Snapshots taken from the simulation of asynchronous cycloaddition mode of stacked benzene and ethylene molecules at (a) 0, (b) 600, (c) 655, (d) 925, (e) 1615, and (f) 1715 fs. The benzene molecule is subjected to the irradiation of a 25 fs (fwhm) laser pulse with a fluence of 94.11 J·m^{-2} and photon energy of 4.7 eV.

results from Geometry II. Here a typical trajectory for each case is reported in this paper.

Some snapshots of the synchronous and asynchronous [2 + 2] photocycloaddition reaction are presented in Figures 2 and 3, respectively. Figure 2(a) shows the equilibrium geometries of benzene and ethylene molecules in the electronic ground state at the moment of excitation. After application of the laser pulse, the benzene molecule is electronically excited and distorted, but the ethylene molecule retains its ground state geometry (Figure 2(b)). Excitation energy is transferred from benzene to ethylene; the two molecules approach each other due and are linked by the synchronous formation of the C_1–C_7 and C_2–C_8 bonds at 730 fs (Figure 2(c)), and ultimately form the cyclobutane type product (Figure 2(d)). The structure of cyclobutane dimer remains stable through the end of the simulation. In Figure 3, the C_1–C_7 bond is formed first (Figure 3(c)) to yield a so-called bonded intermediate (Figures 3(c)–3(e)). The C_2–C_8 bond is later formed to yield the [2 + 2] product (Figure 3(f)).

The HOMO and LUMO are π and π^* orbitals, respectively, and they are initially localized in benzene molecule as illustrated in Figure 4. The variations with time of the HOMO − 1, HOMO, LUMO and LUMO + 1 energies, and the time-dependent population of these molecular orbitals for the synchronous path are presented in Figure 5. Figure 5(a)

shows that the LUMO energy decreases from −2.0 to −2.8 eV and the HOMO energy increases from −7.2 to −7.0 eV after laser excitation and remains more or less constant until 650 fs. At that point, the HOMO and LUMO energy gap narrows sharply to just 0.03 eV at 715 fs; this near-degeneracy suggests an avoided crossing. Thereafter, the gap widens into an average of about 2.6 eV, suggesting the formation of the [2 + 2] product. Figure 5(b) shows that by the end of the laser pulse (which is 50 fs) about 1 electron is excited from the HOMO mainly to the LUMO. This excitation promotes the benzene molecule from the electronic ground state to a low-lying state $\pi\pi^*$. The coupling between the HOMO and LUMO at about 715 fs leads to a transfer of electrons from the LUMO to the HOMO. This deexcitation eventually brings the molecule from the low-lying $\pi\pi^*$ state to the electronic ground state. Shortly, after the avoided crossing, both the LUMO and HOMO levels move back toward their initial values.

Figure 5(c) shows that, in the asynchronous path, two nearly degenerate points are found at 655 and 920 fs, respectively. Figures 5(a) and 5(c) are nearly identical before 655 fs and towards the end of the simulation (after 1600 fs). These suggest the same product formed, but different intermediates are involved in the asynchronous path.
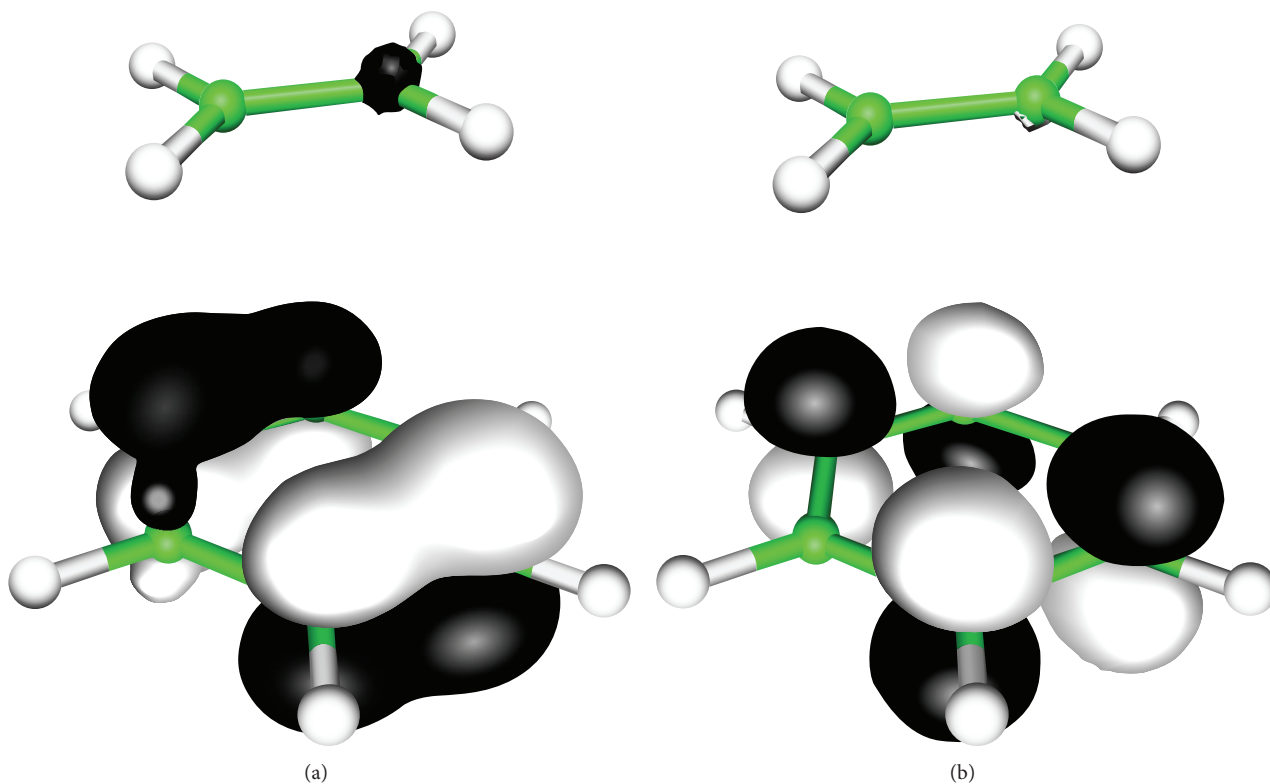
(a)

(b)

FIGURE 4: The diagrams for the HOMO and LUMO of benzene and ethylene molecules at the equilibrated structure computed by the DFTB approximation.

The variations with time of the lengths of the C_1–C_2 and C_7–C_8 bonds and C_1–C_7 and C_2–C_8 distances of both cases are presented in Figure 6. The C_1–C_2 bond is part of a conjugated system and has a bond length of 1.40 Å at the beginning of the simulation; its elongation to about 1.5 Å after the laser pulse was applied suggests conversion to a single bond. Meanwhile, the C_7–C_8 bond length remains essentially constant, suggesting that the ethylene molecule remains in the ground state; only the benzene molecule is affected by the laser pulse. The approach of the excited benzene molecule causes changes in the ethylene as shown by increase in the C_7–C_8 bond length after 650 fs. Both of the C_7–C_8 and C_1–C_2 bond lengths increase to 1.5 Å after 720 fs, consistent with the formation of the cyclobutane dimer. The C_1–C_7 and C_2–C_8 distances are initially 3.5 and 3.6 Å, respectively. They are more or less constant up to 100 fs, slowly decrease until 600 fs, and then sharply shorten to less than 1.6 Å at about 700 fs and 750 fs, respectively. These abrupt changes suggest that the formation of cyclobutane ring involves barrierless pathway. The formation of C_1–C_7 bond and C_2–C_8 bond is about 50 fs apart in the simulation and would be difficult to distinguish experimentally. Thus, the formation of the two bonds may be regarded as a synchronous process.

Figure 7 shows the changes in the C_3–C_2–C_6–C_1 and C_2–C_1–C_7–C_8 dihedral angles with time. The former represents the out-of-plane vibration of benzene ring at C_1 position and the latter corresponds to an overlap of benzene and ethylene moieties. The C_3–C_2–C_6–C_1 dihedral angle

changes indistinctively in synchronous addition mode, even at decay time. This indicates that deformation of C_1 atom has a minimal role in the synchronous mechanism. On the other hand, in the asynchronous addition mode, one can observe a pyramidal geometry at the C_1 site of benzene ring while the other five carbon atoms are almost planar, which resembles the configuration of S_1/S_0 conical intersection of benzene [20] at avoided crossing. It suggests that the out-of-plane vibration of the C_1 atom plays a significant role in nonadiabatic coupling. In synchronous addition mode, the C_2–C_1–C_7–C_8 dihedral angle is always positive, which implies that C_8 atom is outside the hexagonal prism space defined by the vertical projection of the benzene ring through C_7, which leads to poor overlap between benzene and ethylene. However, in asynchronous addition mode, this angle has negative value throughout simulation. It suggests C_8 atom is included in the virtual projection space.

The charge transfers for both cases are presented in Figure 8. During the simulation, no significant charge transfer is observed in the synchronous path. However, the benzene moiety loses about 0.7 electrons at 920 fs, and reversal occurs at 1600 fs in asynchronous mode. This charge transfer at 920 fs indicates that charge transfer plays an important role in the nonadiabatic coupling, which leads to a radiationless transition in asynchronous [2 + 2] photocycloaddition. Furthermore, the charge transfer only occurred after electronic decay, suggesting a zwitterionic intermediate in ground state.
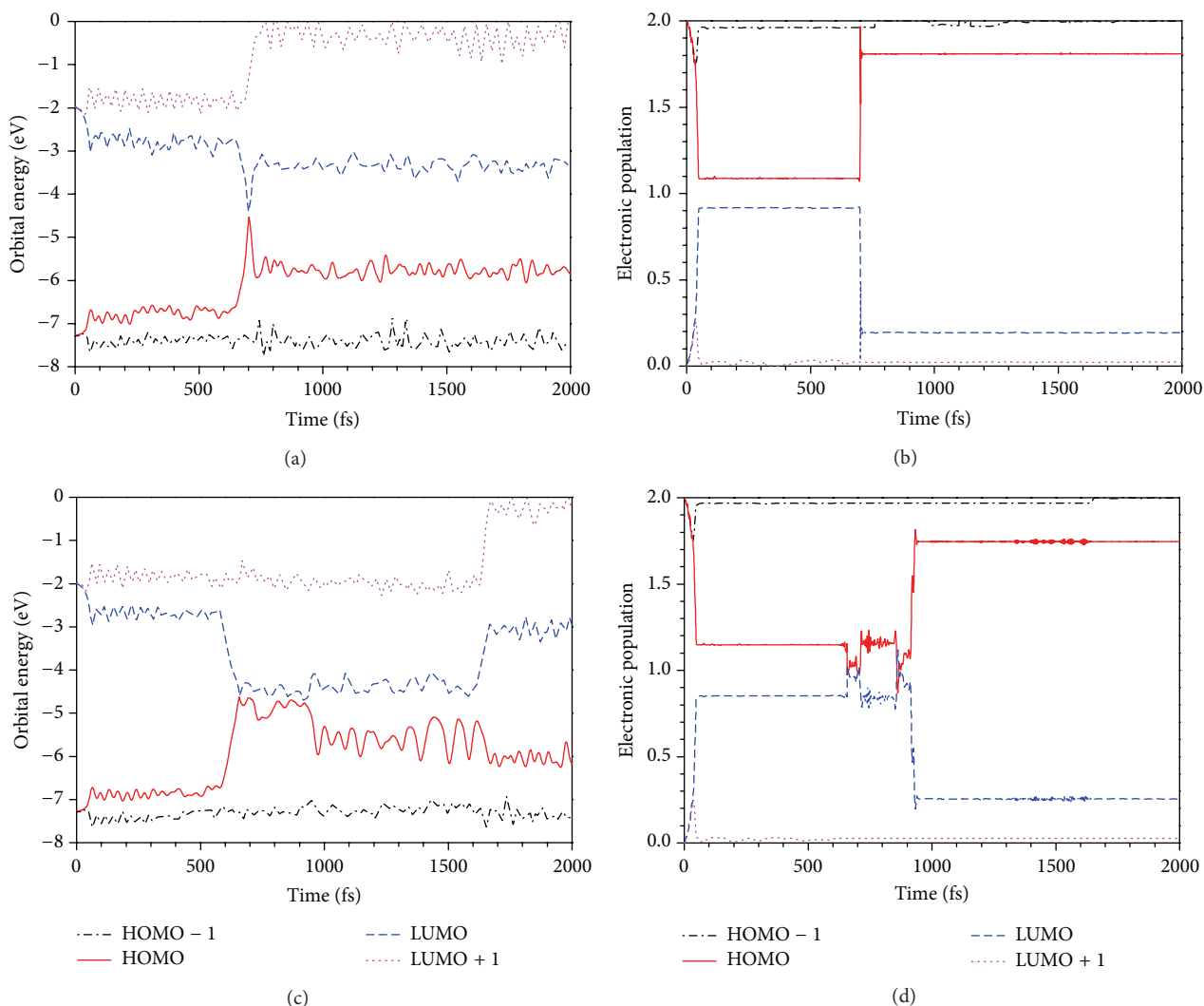
FIGURE 5: The variations with time of (a) the HOMO and LUMO energies; (b) the time-dependent population of stacked benzene and ethylene system in synchronous mode, which is subjected to a laser with frequency of 4.7 eV and fluency of 96.93 J·m^{-2}; (c) and (d) are the HOMO and LUMO energies and the time-dependent population in asynchronous mode, which is subjected to a laser with frequency of 4.7 eV and fluence of 94.11 J·m^{-2}.

Comparison of HOMO and LUMO energy gap with distance between C_2 and C_8 atoms in asynchronous mode is displayed in Figure 9. It is very clear that the energy gap goes through four stages. In stage 1 (50–650 fs), there is little interaction between two moieties because of the relatively large distance, as seen in Figure 6(d). In stage 2 (650–920 fs), C_1 and C_7 linking at 655 fs leads to strong coupling of HOMO and LUMO and the gap sharply narrows to approximately zero. At this timescale, the minimum C_2–C_8 distance reaches 2.2 Å. In consideration of charge transfer not being observed, stage 2 may be defined as "biradical stage." In stage 3 (920–1600 fs), the energy gap increases to about 1 eV. It indicates that a new intermediate is formed. Indeed, stage 3 is in accord with charge transfer shown in Figure 8. The average of C_2–C_8 distance achieves 3.2 Å and the minimum is 2.1 Å during this range. Stage 3 is defined as zwitterionic. In stage 4 (>1600 fs), the electrons transfer back to benzene, and C_2–C_8 bond forms.

In consideration of shortcomings of SERID model, it is also valuable to investigate S_1/S_0 conical intersection in photocycloaddition reaction by using multiconfigurational self-consistent field method. The CASSCF *ab initio* computations used an 8-electron, 8-orbital active space involving all the π orbitals of the benzene and ethylene moieties. It is difficult to optimize CI structure for a system of two interacting molecules because of the difficulty of making a good initial guess. To increase calculation efficiency, we used the geometry at decay time in simulation trajectory as the initial guess for CI optimization. All the CI geometries were optimized using the 6-31G(d) basis set. However, the equilibrated ground state structure of benzene plus ethylene from the simulation was used without any optimization. CASSCF results show that the two conical intersections corresponding to the synchronous and asynchronous mechanisms explicitly exist on the 6-31G(d) potential surface. Their energies (relative to benzene + ethylene in ground state) and some
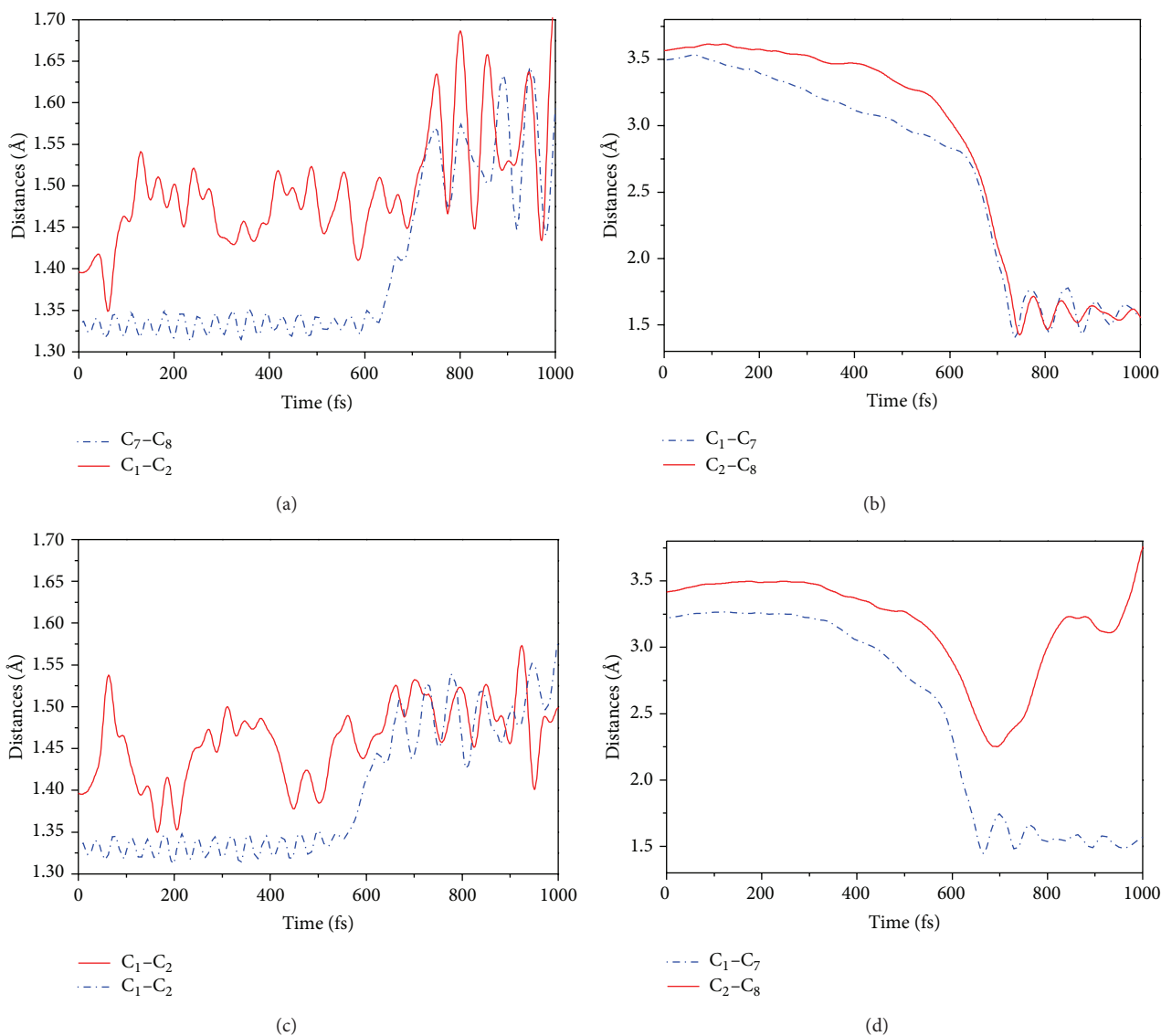
(a)

(b)

(c)

(d)

FIGURE 6: The variations of (a) C_1–C_2 and C_7–C_8 and (b) C_1–C_7 and C_2–C_8 distances with time of synchronous mode. (c) and (d) are these distances in asynchronous mode.

TABLE 1: Energies and geometries of both synchronous and synchronous [2 + 2] photocycloaddition reactions.

Structure	Energy/eV	C_1–C_7/Å	C_2–C_8/Å	C_2–C_1–C_7–C_8/°
S_0 (syn)	0	3.49	3.61	38.2
S_0 (asyn)	0.07	3.22	3.42	−23.6
FC (syn)	4.98	—	—	—
FC (asyn)	4.99	—	—	—
CI (syn)	5.76	2.10	2.06	15.2
CI (asyn)	4.77	1.56	2.66	−38.8

significant geometrical parameters are presented in Table 1. The geometries of CIs, which are very similar to references [5, 6], are displayed in Figure 10.

Although Robb's group had calculated this system by using CASSCF, the overlaps of ethylene moiety and benzene ring in synchronous and asynchronous mode were neglected. Obviously, the $CI_{(syn)}$ with a positive C_2–C_1–C_7–C_8 dihedral of 15.2° indicates an ineffective overlap between two moieties, compared to the initial simulated geometry (Figure 1(a)). In contrast, the $CI_{(syn)}$ has better stacking, with a negative C_2–C_1–C_7–C_8 dihedral angle with value of −38.8°.
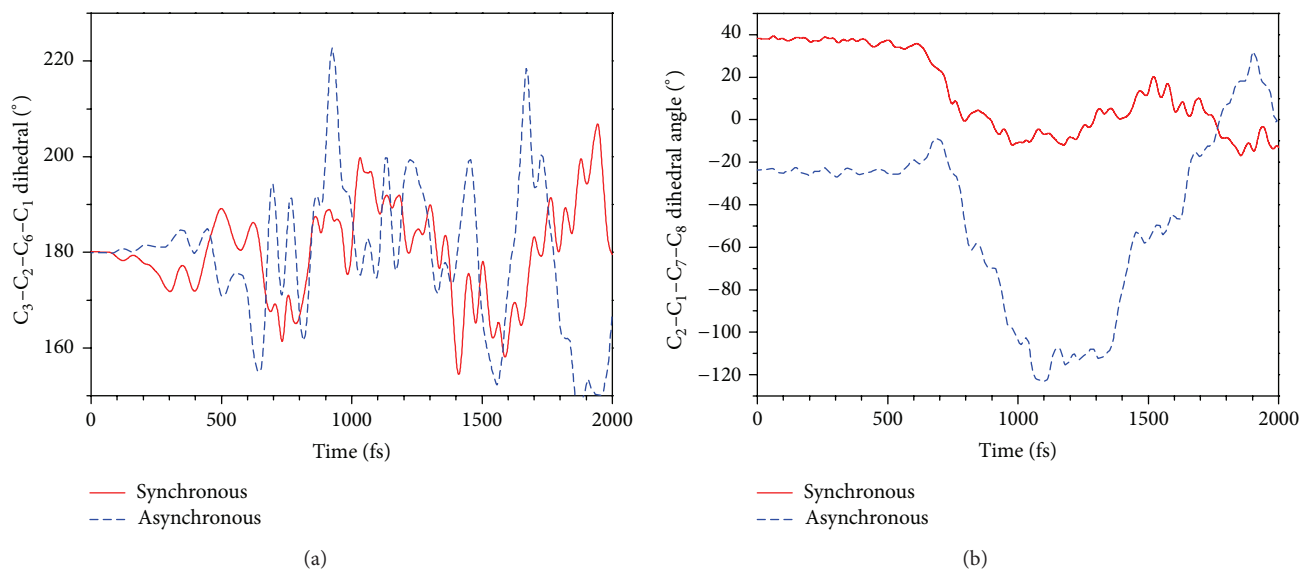
(a)

(b)

FIGURE 7: The variations of dihedral angles (a) $C_3-C_2-C_6-C_1$ and (b) $C_2-C_1-C_7-C_8$ with time for each mode.
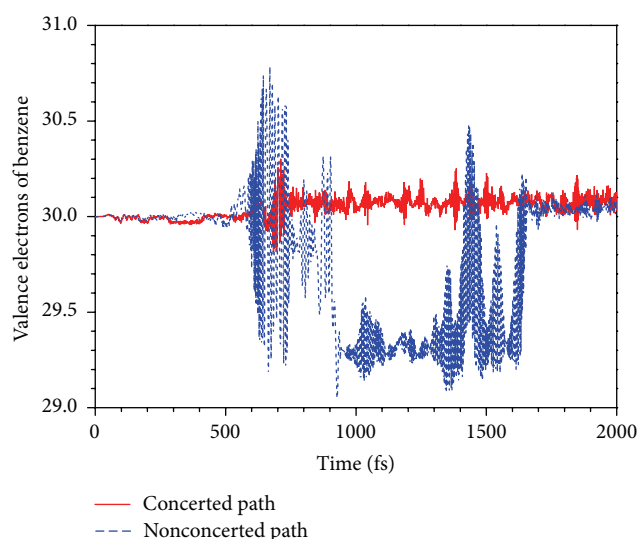

FIGURE 8: The variations of valence electrons of benzene molecule for each photocycloaddition mode.
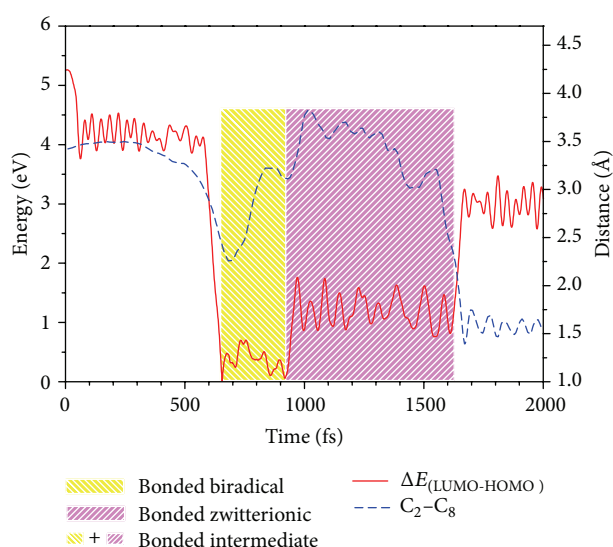

FIGURE 9: Comparison of HOMO and LUMO energy gap and C_2-C_8 distance for asynchronous mode.

The lower energy CI structure belongs to the asynchronous mode; the formation of the C_1-C_7 bond occurs without barrier to yield a low energy conical intersection. Given that benzene could form isomers such as benzvalene and fulvene via an S_1/S_0 conical intersection, the barrier for ethene + benzene cycloaddition must be very small to compete effectively with isomer formation. However, in synchronous mode, the CI energy is even higher than the vertical excitation energy at CASSCF (8,8)/6-31G(d) level. This means that the synchronous photocycloaddition for benzene and ethylene system in S_1 excited state is less accessible.

4. Conclusion

In this paper, we report a semiclassical dynamics simulation study of [2 + 2] cycloaddition reaction of benzene and ethylene induced by ultrashort laser pulses applied to the benzene molecule. When the ethylene molecule is within the vertical projection of benzene shape, excitation leads to a C_1-C_7 bonded intermediate, which evolves to an electroneutral biradical and then to a zwitterionic intermediate at an avoided crossing. Eventually, the electron transfer is reversed as the cycloadduct is formed. Otherwise, a synchronous addition mechanism is observed. In the synchronous mode, the C_1-C_7 and C_2-C_8 form chemical bond simultaneously and no charge transfer is observed.

$\delta(C_8-C_7-C_1-C_2) = 15.2°$

(a)

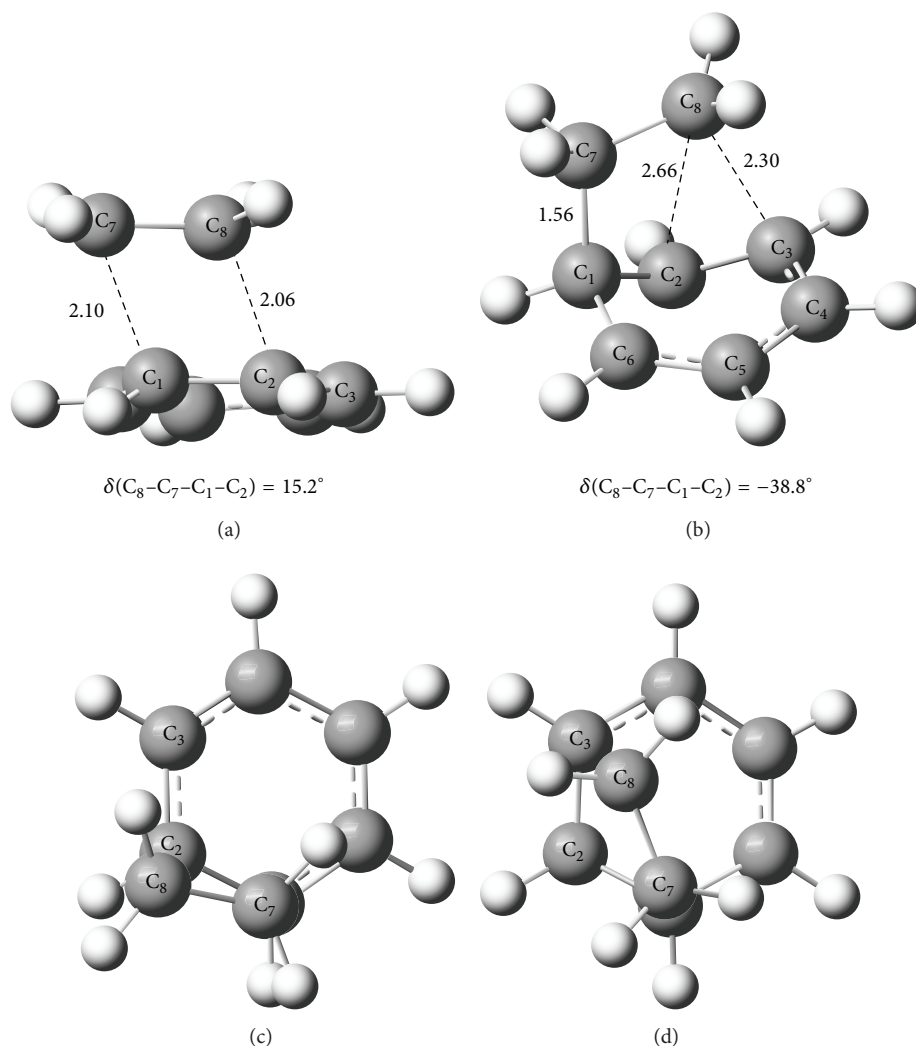$\delta(C_8-C_7-C_1-C_2) = -38.8°$

(b)

(c)

(d)

FIGURE 10: Optimized geometries of S_1/S_0 conical intersection of (a) synchronous and (c) asynchronous mode at CASSCF (8,8)/6-31G(d) level. (b) and (d) are top view of (a) and (c), respectively.

Multiple trajectories simulations show that stacking effect plays an important role in [2 + 2] photocycloaddition reaction of benzene and ethylene molecule. Efficient stacked initial geometry will lead to asynchronous cycloaddition and inefficient stacked initial structure will result in synchronous photoreaction. Statistical results indicate that the quantum yield is higher for the asynchronous mechanism. The CASSCF calculations present that the evolution path from FC to CI is barrierless for asynchronous mode while it has to overcome 0.8 eV barrier in synchronous addition reaction. It suggests asynchronous pathway is a favored predominant pathway for [2 + 2] photocycloaddition reaction between benzene and ethylene, in accord with simulation results.

Conflict of Interests

The authors declare that there is no conflict of interests regarding the publication of this paper.

References

[1] U. Streit and C. G. Bochet, "The arene-alkene photocycloaddition," *Beilstein Journal of Organic Chemistry*, vol. 7, pp. 525–542, 2011.

[2] N. Hoffmann, "Photochemical reactions as key steps in organic synthesis," *Chemical Reviews*, vol. 108, no. 3, pp. 1052–1103, 2008.

[3] D. Bryce-Smith, "Orbital symmetry relationships for thermal and photochemical concerted cycloadditions to the benzene ring," *Journal of the Chemical Society D*, no. 14, pp. 806–808, 1969.

[4] J. A. van der Hart, J. J. C. Mulder, and J. Cornelisse, "Funnels and barriers in the photocycloaddition of arenes to alkenes and dienes," *Journal of Photochemistry and Photobiology A: Chemistry*, vol. 86, no. 1–3, pp. 141–148, 1995.

[5] S. Clifford, M. J. Bearpark, F. Bernardi, M. Olivucci, M. A. Robb, and B. R. Smith, "Conical intersection pathways in the photocycloaddition of ethene and benzene: a CASSCF study with MMVB dynamics," *Journal of the American Chemical Society*, vol. 118, no. 31, pp. 7353–7360, 1996.

[6] J. J. Serrano-Pérez, F. de Vleeschouwer, F. de Proft, D. Mendive-Tapia, M. J. Bearpark, and M. A. Robb, "How the conical intersection seam controls chemical selectivity in the photocycloaddition of ethylene and benzene," *The Journal of Organic Chemistry*, vol. 78, no. 5, pp. 1874–1886, 2013.

[7] C. E. Crespo-Hernández, B. Cohen, and B. Kohler, "Base stacking controls excited-state dynamics in A·T DNA," *Nature*, vol. 436, no. 7054, pp. 1141–1144, 2005.

[8] C. T. Middleton, K. de la Harpe, C. Su, Y. K. Law, C. E. Crespo-Hernández, and B. Kohler, "DNA excited-state dynamics: from single bases to the double helix," *Annual Review of Physical Chemistry*, vol. 60, pp. 217–239, 2009.

[9] W. Zhang, S. Yuan, A. Li, Y. Dou, J. Zhao, and W. Fang, "Photoinduced thymine dimerization studied by semiclassical dynamics simulation," *The Journal of Physical Chemistry C*, vol. 114, no. 12, pp. 5594–5601, 2010.

[10] S. Yuan, W. Zhang, L. Liu, Y. Dou, W. Fang, and G. V. Lo, "Detailed mechanism for photoinduced cytosine dimerization: a semiclassical dynamics simulation," *Journal of Physical Chemistry A*, vol. 115, no. 46, pp. 13291–13297, 2011.

[11] Y. Dou, B. R. Torralva, and R. E. Allen, "Semiclassical electron-radiation-ion dynamics (SERID) and cis-trans photoisomerization of butadiene," *Journal of Modern Optics*, vol. 50, no. 15-17, pp. 2615–2643, 2003.

[12] Y. Dou, B. R. Torralva, and R. E. Allen, "Interplay of electronic and nuclear degrees of freedom in a femtosecond-scale photochemical reaction," *Chemical Physics Letters*, vol. 392, no. 4–6, pp. 352–357, 2004.

[13] M. Lein, T. Kreibich, E. K. U. Gross, and V. Engel, "Strong-field ionization dynamics of a model H_2 molecule," *Physical Review A: Atomic, Molecular, and Optical Physics*, vol. 65, Article ID 033403, 2002.

[14] S. Chelkowski, T. Zuo, O. Atabek, and A. D. Bandrauk, "Dissociation, ionization, and Coulomb explosion of $H2^+$ in an intense laser field by numerical integration of the time-dependent Schrödinger equation," *Physical Review A*, vol. 52, no. 4, pp. 2977–2983, 1995.

[15] D. Porezag, T. Frauenheim, T. Köhler, G. Seifert, and R. Kaschner, "Construction of tight-binding-like potentials on the basis of density-functional theory: application to carbon," *Physical Review B*, vol. 51, no. 19, pp. 12947–12957, 1995.

[16] M. Elstner, D. Porezag, G. Jungnickel et al., "Self-consistent-charge density-functional tight-binding method for simulations of complex materials properties," *Physical Review B*, vol. 58, no. 11, pp. 7260–7268, 1998.

[17] J. Frank, *Introduction to Computational Chemistry*, John Wiley & Sons, Chichester, UK, 2007.

[18] C. J. Cramer, *Essentials of Computational Chemistry*, John Wiley & Sons, Chichester, UK, 2002.

[19] M. J. Frisch, G. W. Trucks, H. B. Schlegel et al., *Gaussian 09, Revision D.01*, Gaussian, Wallingford, Conn, USA, 2010.

[20] L. J. Palmer, L. N. Ragazos, F. Bernardi, M. Olivucci, and M. A. Robb, "An MC-SCF study of the S1 and S2 photochemical reactions of benzene," *Journal of the American Chemical Society*, vol. 115, no. 2, pp. 673–682, 1993.